

Analytical and Experimental Assessment of Two Methods of Determining Turbine Efficiency

Susan T. Hudson*

NASA Marshall Space Flight Center, Huntsville, Alabama 35812

and

Hugh W. Coleman†

University of Alabama in Huntsville, Huntsville, Alabama 35899

The efficiency of a turbine may be calculated from measured test variables by several different methods. However, the literature does not contain documentation to aid one in determining the preferred efficiency method for particular test situations. Two methods commonly used for cold airflow testing of turbines, the thermodynamic and the mechanical methods, were evaluated both experimentally and using uncertainty analysis techniques. The experimental work involved performance testing of a next-generation, compact, high-turning-angle turbine design in which the flow contained significant high-gradient regions. The turbine efficiency was calculated from the measured test data using both efficiency methods, and enhanced uncertainty analysis tools were developed to evaluate the efficiency uncertainty for each method. The efficiency uncertainty equations were written in a new form to account properly for conceptual bias and correlated bias terms. The results showed that using the form of the equations developed was essential to obtaining the correct efficiency uncertainty estimates. The efficiency uncertainty estimates obtained from the analysis then allowed a comparison of the two methods from which conclusions were drawn to guide in determining the preferred efficiency method for individual applications.

Nomenclature

B	= bias limit estimate
C_p	= specific heat at constant pressure, Btu/lbm °R
h	= enthalpy, Btu/lbm
J	= conversion constant, 778.3 ft-lbf/Btu
K	= conversion constant, $\pi/30$ rad · min/revolution · s
N	= number of readings or speed, rpm
P	= pressure, psia
Pr	= pressure ratio (total-to-total)
r	= result
S	= sample standard deviation
T	= temperature, °R
Tq	= torque, ft-lbf
U	= uncertainty estimate
\dot{W}	= mass flow rate, lbm/s
X	= variable
α	= flow or yaw angle
γ	= ratio of specific heats
η	= efficiency
θ	= sensitivity coefficient

Subscripts

me	= mechanical method
th	= thermodynamic method
0	= total

1	= turbine inlet
2	= turbine exit

Introduction

COMPONENT testing of turbines is needed to characterize the aerodynamic performance of the machine. This type of testing is useful for new turbine designs attempting to incorporate advanced technologies as well as for existing engine turbine designs. Component testing is often done in air at scaled conditions so that the turbine can be tested over a broad operating range at lower risk.¹ The test results are used to improve the turbine design and validate various computer codes used for design and performance prediction.

When preparing for a turbine test, one must be aware of the uncertainty limits required for the results and must plan the test to meet these uncertainty requirements. Often there are several methods available for obtaining the needed result. Several variations of the basic equation for turbine efficiency may be used in turbine performance testing. The particular equation used depends on the type of test facility, the types of measurements that are available, etc. However, a literature survey revealed little documentation of uncertainty analyses evaluating differences in methods used to calculate turbine efficiency from the measured test variables.² This type of analysis is needed to determine how to approach a test, the measurements required, etc. Two common methods used to determine turbine efficiency for cold airflow turbine testing were evaluated in this study, both experimentally and using uncertainty analysis techniques.

The work was prompted by a research program involving the testing of a subscale rocket turbine that required that the turbine efficiency be determined within 1% ($U_\eta/\eta \times 100 \leq 1\%$). The efficiency uncertainty requirement forced a study of the turbine efficiency methods and the measurements involved. The turbine efficiency methods were evaluated on several different levels. A general uncertainty analysis was performed to compare the two efficiency methods and to evaluate the relative importance of the uncertainty of each of the measured variables on the uncertainty of the efficiency.^{3,4} These results were used to plan the test and design new instrumentation calibration approaches necessary if the test objective was to be met.^{3,5} Once the test proceeded past the planning phase, the necessary calibrations were conducted and detailed uncertainty analyses were performed for the various measurements needed to

Presented as Paper 98-2711 at the AIAA 20th Advanced Measurement and Ground Testing Technology Conference, Albuquerque, NM, 15–18 June 1998; received 2 November 1998; revision received 28 April 1999; accepted for publication 1 June 1999. Copyright © 1999 by the American Institute of Aeronautics and Astronautics, Inc. No copyright is asserted in the United States under Title 17, U.S. Code. The U.S. Government has a royalty-free license to exercise all rights under the copyright claimed herein for Governmental purposes. All other rights are reserved by the copyright owner.

*Aerospace Engineer, Space Transportation Directorate, TD63, Senior Member AIAA.

†Eminent Scholar in Propulsion and Professor, Propulsion Research Center, Department of Mechanical and Aerospace Engineering, Associate Fellow AIAA.

determine turbine efficiency.^{6–9} Once the test data were obtained, they were used in a detailed uncertainty analysis to determine the uncertainty in the turbine efficiency and further evaluate the efficiency methods.

This paper focuses on the detailed uncertainty analysis of the turbine efficiency methods and how these results can be used to determine the preferred method for particular test situations. The turbine efficiency methods will be presented first. A brief uncertainty analysis overview and a description of the experimental turbine test case will follow to provide the necessary background information. The detailed uncertainty analysis will then be discussed. The results from the analysis will be used to evaluate the two efficiency methods and to provide information on choosing the appropriate method for individual applications. The turbine efficiency methods have not been evaluated in this manner in the past.

Turbine Efficiency Methods

Two equations were used to calculate turbine efficiency from measured test variables during this study.^{2,10} Both equations are derived from the basic definition of turbine efficiency: actual enthalpy change over ideal or isentropic enthalpy change. Both methods are used for cold airflow turbine testing, where the temperature is relatively low so that an ideal gas may be assumed and γ and C_p are considered constant.

For the first method, the thermodynamic method, the temperature drop across the turbine is measured to determine the actual enthalpy change ($\Delta h = C_p \Delta T$). Isentropic relations are used to write the ideal enthalpy change in terms of turbine inlet and exit total pressure rather than temperature. With the preceding assumptions, the equation for thermodynamic efficiency becomes

$$\eta_{th} = \frac{T_{01} - T_{02}}{T_{01} \left[1 - (P_{02}/P_{01})^{(\gamma-1)/\gamma} \right]} \quad (1)$$

For the second method, the mechanical method, the ideal enthalpy change is calculated the same as before. However, the mechanical measurements of torque and speed are used along with the measured mass flow rate to determine the actual enthalpy change. The efficiency equation is

$$\eta_{me} = \frac{K T q N}{J C_p \dot{W} T_{01} \left[1 - (P_{02}/P_{01})^{(\gamma-1)/\gamma} \right]} \quad (2)$$

Note that the temperatures and pressures required for Eqs. (1) and (2) are average values at a cross section.

Uncertainty Analysis Overview

Only a brief overview of the methodology to obtain uncertainty estimates and how they propagate through a given data reduction equation is given here. The reader is referred to Coleman and Steele for a detailed discussion of uncertainty analysis techniques.^{11,12}

The word accuracy is generally used to indicate the relative closeness of agreement between an experimentally determined value of a quantity and its true value. Error is the difference between the experimentally determined value and the truth; therefore, as error decreases, accuracy is said to increase. Only in rare instances is the true value of a quantity known. Thus, it is necessary to estimate error, and that estimate is called an uncertainty U . Uncertainty estimates are made at some confidence level; a 95% confidence estimate, for example, means that the true value of the quantity is expected to be within the $\pm U$ interval about the experimentally determined value 95 times out of 100.

Total error can be considered to be composed of two components: a precision (random) component ε and a bias (systematic) component β . An error is classified as precision if it contributes to the scatter of the data; otherwise, it is a bias error. As an estimator of β , a systematic uncertainty or bias limit B is defined. A 95% confidence estimate is interpreted as the experimenter being 95% confident that the true value of the bias error, if known, would fall within $\pm B$. A useful approach to estimating the magnitude of a bias error is to assume that the bias error for a given case is a single realization drawn from some statistical parent distribution of possible

bias errors. In other words, the bias error could be treated as a random variable, but with only a single realization, its variance cannot be measured and must be estimated. As an estimator of the magnitude of the precision errors, a precision uncertainty or precision limit P for a single reading is defined. A 95% confidence estimate of P is interpreted to mean that the $\pm P$ interval about the single reading of X_i should cover the (biased) parent population mean μ , 95 times out of 100.

In nearly all experiments, the measured values of different variables are combined using a data reduction equation (DRE) to form some desired result. A general representation of a data reduction equation is

$$r = r(X_1, X_2, \dots, X_J) \quad (3)$$

where r is the experimental result determined from J measured variables X_i . Each of the measured variables contains bias errors and precision errors. These errors in the measured values then propagate through the DRE, thereby generating the bias and precision errors in the experimental result r .

The 95% confidence expression for U_r is

$$U_r^2 = B_r^2 + P_r^2 \quad (4)$$

If the large sample assumption is made ($N \geq 10$) (Ref. 12), the systematic uncertainty (bias limit) of the result is defined as

$$B_r^2 = \sum_{i=1}^J \theta_i^2 B_i^2 + 2 \sum_{i=1}^{J-1} \sum_{k=i+1}^J \theta_i \theta_k B_{ik} \quad (5)$$

where

$$\theta_i = \frac{\partial r}{\partial X_i} \quad (6)$$

The bias limit estimate for each X_i variable is the root sum square combination of its elemental systematic uncertainties

$$B_i = \left[\sum_{j=1}^M (B_i)_j^2 \right]^{1/2} \quad (7)$$

and B_{ik} , the 95% confidence estimate of the covariance appropriate for the bias errors in X_i and X_k , is determined from

$$B_{ik} = \sum_{\alpha=1}^L (B_i)_\alpha (B_k)_\alpha \quad (8)$$

where variables X_i and X_k share L identical error sources. These terms account for correlation between bias errors in different measurements. More detailed discussions of the covariance approximation are given in Refs. 13–15.

The precision uncertainty (precision limit) of the result is

$$P_r^2 = \sum_{i=1}^J \theta_i^2 P_i^2 + 2 \sum_{i=1}^{J-1} \sum_{k=i+1}^J \theta_i \theta_k P_{ik} \quad (9)$$

where P_{ik} is the 95% confidence estimate of the covariance appropriate for the precision errors in X_i and X_k . The 95% confidence large sample ($N \geq 10$) precision limit for a variable is estimated as

$$P_i = 2S_i \quad (10)$$

where S_i is the sample standard deviation.

Typically, correlated precision uncertainties have been neglected so that the P_{ik} terms in Eq. (9) are taken as zero. These covariance terms account for correlation between errors in different measurements. The precision errors have been considered to be random; therefore, the correlation between them has been assumed to be zero. That assumption is true in the work reported here; however, a case is presented in Refs. 3 and 6 where the precision errors are correlated and the covariance terms are important.

A general uncertainty analysis for this turbine test case was performed previously. There, the uncertainties of the variables were not considered separately in terms of bias and precision.⁴ An estimate of the overall uncertainty of each variable was made. These uncertainty values were then propagated through the DREs [Eqs. (1) and

(2) for this case]. In this study a detailed uncertainty analysis in which bias and precision are considered separately has been implemented. Because the pressures and temperatures in Eqs. (1) and (2) are averages determined from many point measurements, the uncertainty analysis is complex inasmuch as there are many B_{ik} terms that must be included. Also, the conceptual bias that arises when the measured variables (point measurements at different spatial locations) do not correspond to the variables required in the equations (average values at a cross section) is important.

Description of Experiment

The experimental test case used for this study was a liquid rocket engine turbine test model called the oxidizer technology turbine rig (OTTR).^{16,17} This model was designed to be tested in NASA Marshall Space Flight Center's (MSFC's) cold airflow turbine test facility,¹⁸ which is a blowdown facility that operates by expanding high-pressure air (420 psig) from one or two 6000-ft³ air tanks to atmospheric conditions. Air flows from the storage tanks through a heater section, quiet trim control valve, and a calibrated subsonic mass flow venturi. Flow then continues through the test model and backpressure valve and exhausts to atmosphere. The facility can accommodate axial flow, radial inflow, and radial outflow turbines.

This equipment can deliver up to 220-psia air for run times from 30 s to over 1 h, depending on inlet pressure and mass flow rate. The heater allows a blowdown-controlled temperature between 530 and 830°R. The facility has manual setpoint closed-loop control of the model inlet total pressure, inlet total temperature, shaft rotational speed, and pressure ratio. In addition to these control parameters, the facility can accurately measure mass flow, torque, and horsepower. The associated data system is capable of measuring 512 pressures, 120 temperatures, and several model health-monitoring variables.

The OTTR was designed to support the development of advanced turbines for future liquid rocket engines. It is a highly loaded single-stage liquid-oxygen pump drive turbine that uses inlet and exit volutes to provide optimum performance in a compact configuration (Figs. 1 and 2). The system design creates high pressure and temperature gradients as well as high Mach number flow (nominally 0.8 at the turbine exit). These factors make it especially difficult to measure the flowfield accurately. However, the need to use the OTTR test data both for performance evaluation and for computational fluid dynamics code validation resulted in strict accuracy requirements for the data ($U_\eta/\eta \times 100 \leq 1\%$). The accuracy requirement coupled with the complicated flowfield of the OTTR forced a detailed investigation of all of the facility and test rig measurements. Several test issues were identified as crucial to obtaining accurate test data.^{3,5} Therefore, instrumentation was chosen and measurement procedures were developed to reduce the uncertainty of the critical measurements and to meet the OTTR test goals.

The OTTR was very highly instrumented, but only the turbine inlet and exit instrumentation is of interest here. Automatic circumferential traverse gears were used to rotate instrumentation rings at the turbine inlet and exit planes. These traverse gears could remotely move the rings through 90 deg. Each of the rings could accommodate a total of eight rakes and two probes with radial actuators. Each rake contained five probes (total pressure or total temperature) positioned

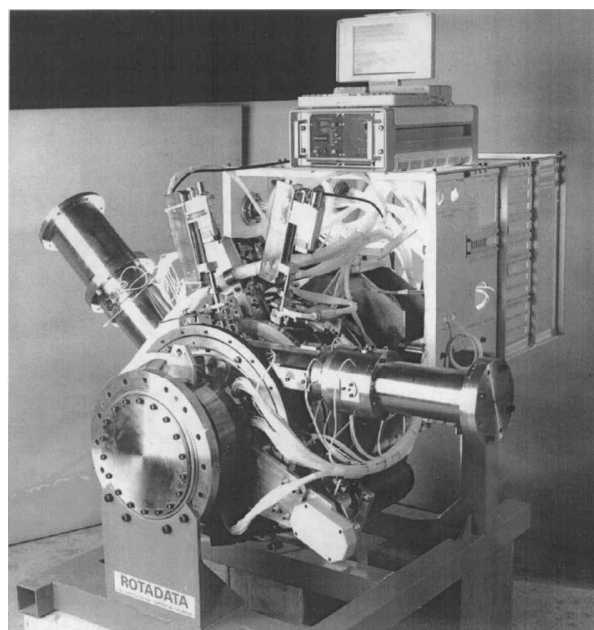


Fig. 2 OTTR.

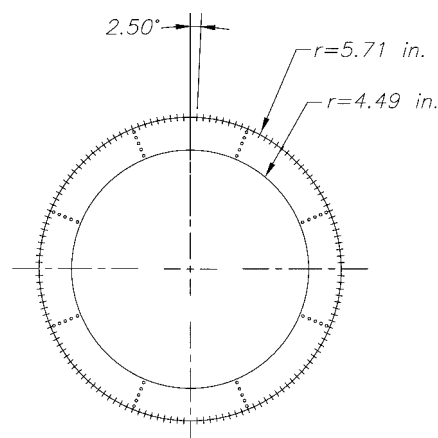


Fig. 3 Turbine inlet and exit plane measurement locations.

on centers of equal area. These rakes could be manually adjusted for yaw angle. Contoured plugs were available for each rake position, and these were inserted when a rake was not being used. The probes used with the radial actuators were three-hole cobra probes. These cobra probes were run in the autonulling mode. Because the cobra probes on radial actuators could only map 180 deg of the turbine plane, a modified prism probe (YC probe) was adapted to map the remaining 180 deg. This probe could be placed in any of the eight rake positions. The YC probe had to be used in a fixed position (rather than autonulling); it could be manually adjusted for both radial position and yaw angle. Details on the OTTR instrumentation are given in Refs. 3, 5, and 17.

The turbine inlet flowfield was mapped using the total pressure and total temperature rakes. Measurements were made at five radial locations, on centers of equal area, every 2.5 deg. This resulted in 720 point measurements of pressure and temperature at the turbine inlet plane. The turbine exit flowfield was mapped with the total pressure and total temperature rakes as well as with three-hole probes (cobra and YC) to obtain static pressure and flow angle. Again, measurements were made at 720 points (five radial positions every 2.5 deg). The circumferential location is defined with top dead center at 0 deg and moving clockwise looking downstream. The radial position is described as percent span with 0% being the hub and 100% being the tip. The eight rakes with their five radial probes are shown in Fig. 3. The circumferential angles are marked every 2.5 deg to show the density of the measurements made. The number

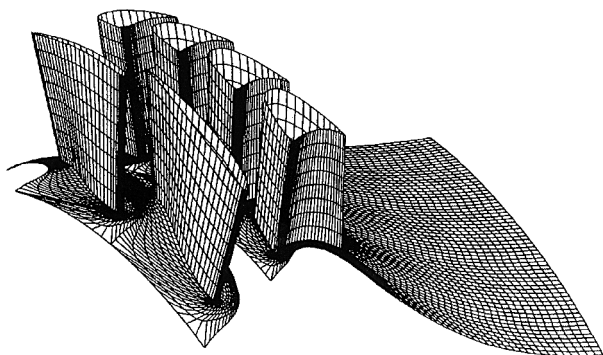


Fig. 1 OTTR vanes and blades.

of measurements made (720) was based on the size of the probes and flowpath because no pretest analysis technique was available to determine the optimum number of measurements required to meet the test goals.

The P_0 , P , T_0 , α , and \dot{W} distributions resulting from the 720 point measurements showed that the turbine inlet quantities could be area averaged because the gradients were fairly small. However, because of the large gradients in the turbine exit flowfield, the turbine exit quantities needed to be mass averaged to obtain the proper values. The averaging procedures and the effect of these gradients on turbine performance are discussed in detail in Ref. 3.

The model measurements, discussed earlier, combined with the facility measurements of mass flow rate, torque, and speed provided the information necessary to calculate turbine efficiency by both the thermodynamic [Eq. (1)] and mechanical [Eq. (2)] methods.

Testing of the OTTR was done at the turbine aerodynamic design point (ADP) as well as over a broad offdesign operating envelope. The setpoint parameters for the test were the turbine inlet total pressure, inlet total temperature, speed, and total-to-total pressure ratio. Results presented here will only be for the aerodynamic design point: $P_{01} = 100$ psia, $T_{01} = 560^\circ\text{R}$, $N = 3710$ rpm, and $Pr = 1.60$.

Description of Analysis

Procedure

Once the test data were taken, a posttest detailed uncertainty analysis was done to evaluate the uncertainty of the efficiency calculated by the thermodynamic and mechanical methods for the OTTR ADP. The uncertainty estimates used for the detailed analysis were refined from the general analysis, mentioned earlier, based on new calibration, measurement, and data acquisition techniques developed for the high-gradient regions as a result of information gained from the general analysis.^{3,4} Uncertainty analysis methods were developed for the detailed analysis to account for the averaging procedures used explicitly. This was done to reduce the conceptual bias that arises when the measured variables do not correspond to the variables required in the equations and resulted in numerous correlation terms that arise when errors in measurements are correlated. Note, however, that this work was limited to the uncertainty of the efficiency determined from the air test. Therefore, uncertainties in efficiency due to testing a turbine in air and then using these results for a turbine that will operate in an engine with a different fluid were not addressed. To apply air test results to an engine, differences in gas thermodynamic properties and differences in geometric dimensions due to higher operating temperatures must be considered.¹⁹

The detailed analysis began with the equations for turbine efficiency [Eqs. (1) and (2)] as the data reduction equations. The basic equations for uncertainty, bias, and precision were Eqs. (4), (5), and (9), respectively. From Eq. (1), η_{th} is a function of P_{01} , P_{02} , T_{01} , T_{02} , and γ . From Eq. (2), η_{me} is a function of P_{01} , P_{02} , T_{01} , \dot{W} , Tq , N , γ , C_p , J , and K . The uncertainties of the conversion constants, J and K , were considered negligible. Work was done early in the OTTR test program to evaluate the effect of uncertainties in γ and C_p on the uncertainty of the turbine efficiency. The analysis results showed that the effects of the uncertainties of γ and C_p were negligible relative to the effects of the uncertainties of the measured pressures, temperatures, mass flow rate, torque, and speed for this case. (This may not be true for all operating conditions and should be checked for each case.) Therefore, η_{th} is a function of P_{01} , P_{02} , T_{01} , and T_{02} , and η_{me} is a function of P_{01} , P_{02} , T_{01} , \dot{W} , Tq , and N for the OTTR. However, the turbine inlet and exit quantities were averages of 720 point measurements, and the static pressure and flow angle were required to mass average the exit quantities. Therefore,

$$\eta_{th} = \eta_{th} \left[\sum_{i=1}^{720} (P_{01}, P_{02}, T_{01}, T_{02}, P_2, \alpha_2)_i \right] \quad (11)$$

and

$$\eta_{me} = \eta_{me} \left[\dot{W}, Tq, N, \sum_{i=1}^{720} (P_{01}, P_{02}, T_{01}, P_2, \alpha_2)_i \right] \quad (12)$$

Combining Eq. (11) with Eqs. (4), (5), and (9) gives the uncertainty in the thermodynamic efficiency (see the Appendix). Combining Eq. (12) with Eqs. (4), (5), and (9) gives the uncertainty in the mechanical efficiency (Appendix).

These efficiency uncertainty equations (Appendix) have not been written in this form in the past. Previously, only one term was used for each variable in the DRE regardless of the number of point measurements made to obtain the value of the variable for the DRE. The form presented here explicitly accounts for the number of point measurements made and the averaging procedures used. This method properly accounts for the conceptual bias and the correlated bias terms.

In the $U_{\eta_{th}}$ equation (Appendix), terms 1–6 on the right-hand side are the precision terms for each variable, terms 7–12 are the bias terms for each variable, terms 13–18 are the correlated bias terms between point measurements of the same variable, and terms 19–25 are the correlated bias terms for the point measurements of different variables. In the $U_{\eta_{me}}$ equation (Appendix), terms 1–8 on the right-hand side are the precision terms for each variable, terms 9–16 are the bias terms for each variable, terms 17–21 are the correlated bias terms between point measurements of the same variable, and terms 22–27 are the correlated bias terms for the point measurements of different variables. Based on past experience with the test facility and data acquisition systems, all correlated precision terms were assumed to be zero.³

In writing the uncertainty equations, the following assumptions were made concerning correlated bias terms. All of the pressure measurements (P_{01} , P_{02} , and P_2) were correlated because all were measured on the same electronic pressure scanning system and were calibrated against the same standard. All of the temperature measurements (T_{01} and T_{02}) were correlated because all thermocouples were calibrated against the same standard. A worst-case sensitivity study showed that the effect of the correlation terms for pressures with flow angles on the efficiency uncertainty was negligible; therefore, these values were set to zero. The pressure and temperature measurements, as well as the flow angle and temperature measurements, were considered uncorrelated. No correlation terms were considered for the facility measurements of mass flow rate, torque, and speed.

See Refs. 3 and 20 for more details on the analytical procedure.

Uncertainty Estimates

Uncertainty estimates were needed for all of the measured variables. Table 1 lists the estimates needed for the uncertainty equations. (See Ref. 3 for details on deriving these estimates.) The uncertainties for P_2 and α_2 vary depending on whether the cobra probe was used, the YC probe was used, or a curve fit of the data was used to obtain these values. Notice that when regression analyses¹³ were used to evaluate the uncertainty of a measurement (T_{02} , P_2 , and α_2), separate bias and precision limits are not given; only an overall uncertainty estimate is given. This was done because the regression analyses combine bias and precision from calibration and test data into an overall uncertainty estimate. It is not useful to try to separate these into bias and precision. The bias and precision terms in the

Table 1 Uncertainty estimates

Variable, X	P_X	B_X	U_X	Variables, $X_i X_j$	$B_{X_i X_j}$
$(P_{01})_i$, psia	0.15	0.11	—	$P_{01} P_{01}$, psia	0.013
$(T_{01})_i$, °R	0.71	0.18	—	$T_{01} T_{01}$, °R	0.023
$(P_{02})_i$, psia	0.15	0.11	—	$P_{02} P_{02}$, psia	0.013
$(T_{02})_i$, °R	—	—	0.74	$T_{02} T_{02}$, °R	0.023
$(P_2)_{i, cobra}$, psia	—	—	0.30	$P_2 P_2$, psia	0.013
$(P_2)_{i, YC}$, psia	—	—	0.36	$(\alpha_2 \alpha_2)_{cobra}$, deg	0.250
$(P_2)_{i, curve fit}$, psia	—	—	0.54	$(\alpha_2 \alpha_2)_{YC}$, deg	0.810
$(\alpha_2)_{i, cobra}$, deg	—	—	0.50	$P_{01} P_{02}$, psia	0.013
$(\alpha_2)_{i, YC}$, deg	—	—	0.90	$P_{01} P_2$, psia	0.013
$(\alpha_2)_{i, curve fit}$, deg	—	—	1.00	$P_{02} P_2$, psia	0.013
\dot{W} , lbm/s	—	—	0.089	$T_{01} T_{02}$, °R	0.023
Tq , ft-lbf	0.11	0.70	—		—
N , rpm	0.42	1.00	—		—

uncertainty equations were combined into one uncertainty term for these three variables. The elemental error due to averaging using a finite number of measurements instead of integrating a continuous function was considered negligible relative to the other elemental sources because such a large number of points were measured in the inlet and exit planes. In a situation with fewer measurements, this elemental source could be significant.

Note that the estimate used for the uncertainty of the torque is for the torque measurement only. When calculating turbine efficiency for the rig test, the torque that the turbine blading produces is the value needed. This value will be higher than the measured torque due to rig losses (bearings, disk windage, etc.). It is standard to add a tare torque correction to the measured torque to obtain the torque value required to calculate efficiency.¹⁰ Therefore, the torque value required for Eq. (2) is actually

$$Tq = Tq_{\text{measured}} + Tq_{\text{tare}} \tag{13}$$

Because of a lack of funding, a tare test to measure the torque correction for the OTTR was not possible. When the OTTR test was being planned, a tare test on a core module (shaft and bearing assembly) of the same design as the OTTR core module was expected to be run. It was agreed (private communication with P. D. Johnson and F. W. Huber, Pratt and Whitney, West Palm Beach, Florida, 1994) that the results from this test could be used to account for all effects except disk windage¹⁰ for the OTTR tare torque correction. Disk windage would be estimated from analysis and combined with the tare test results to determine the overall correction for the OTTR. Unfortunately, this tare test was cancelled. Therefore, no value for the OTTR tare torque has been decided on at the present time. Once this number is derived, it must be added to the measured torque to calculate efficiency by the mechanical method. The torque bias limit must then be updated because the torque bias limit used in this work was estimated with Tq_{tare} assumed as zero. Accounting for the tare torque will increase the turbine efficiency calculated by the mechanical method, and accounting for the bias associated with the tare torque will increase the uncertainty of the efficiency calculated by the mechanical method.

The covariance estimates needed for the uncertainty equations are also given in Table 1. The covariance estimate is the sum of the products of the bias limits of the elemental sources that are common between the two measurements [Eq. (8)]. For all of the pressure terms, the elemental sources attributed to the electronic pressure scanning system dominated all other sources; therefore, the covariance approximations were the same (0.013 psi) for all of these terms. For the temperature measurements, the bias of the standard used for the static calibration⁷ was the only correlated elemental source; therefore, all of these covariance terms were equal (0.023°R). The covariance approximations for $\alpha_2\alpha_2$ varied depending on the region and the instrument used to make the measurement.³

Results

A FORTRAN code was written to calculate the uncertainty in the turbine efficiency for both the thermodynamic and mechanical methods using the procedures and uncertainty estimates discussed in the preceding sections. Input for the code included 720 measurements of P_{01} , P_{02} , T_{01} , T_{02} , P_2 , and α_2 along with the average values of \dot{W} , Tq , and N at the OTTR ADP. The uncertainty estimates given in Table 1 were also input for the code. Efficiency was then calculated from the test data using Eqs. (1) and (2) with the proper averaging techniques for the turbine inlet and exit quantities. The uncertainty in the efficiency was calculated for both methods using the uncertainty equations given in the Appendix. A central difference numerical scheme was used to compute the partial derivatives. Output from the code is given in Table 2. The output includes the average turbine inlet and exit quantities, the facility measurements, the efficiency by both methods, and the uncertainty in the efficiency for both methods.

The uncertainty percentage contribution (UPC) values are also given in Table 2 for each term for both efficiency methods. These terms are used to evaluate the sensitivity of the uncertainty of the result (efficiency) to the uncertainty of the various measured quantities. The UPC is defined as

$$UPC_i = (\theta_i U_i)^2 / U_r^2 \times 100 \tag{14}$$

or

$$UPC_{ik} = (2\theta_i \theta_k B_{ik}) / U_r^2 \times 100 \tag{15}$$

with θ defined in Eq. (6). The UPC illustrates the influence of each variable and its uncertainty as a percent of the result uncertainty squared for each term in the uncertainty equation. This approach shows the sensitivity of the squared uncertainty of the result to the squared uncertainty effect of each of the variables for a particular situation where values for the variables are known and the uncertainties for each variable have been estimated. The values given in Table 2 are the summations of all point measurement UPCs for a variable and its associated correlation terms.

The efficiency calculated with the thermodynamic method using mass averaged exit conditions was 0.646 or 64.6%. The mechanical method efficiency was 0.603 or 60.3%. The two methods differ by 0.043 points. This difference is large because the turbine torque has not been corrected for tare losses, as discussed earlier. A tare torque correction, when applied, will increase the mechanical efficiency, thus reducing the difference between the two methods.

The uncertainty in the efficiency was less for the thermodynamic method ($\approx 0.2\%$ in η) than for the mechanical method ($\approx 0.8\%$ in η with the tare torque and its uncertainty ignored). Both methods appeared to have met the uncertainty goal of 1% at the ADP; however, the mechanical method analysis is incomplete due to the tare

Table 2 Results

Performance results		Thermodynamic method UPC			Mechanical method UPC		
Variable	Value	Term	UPC	Sum of all terms for a variable	Term	UPC	Sum of all terms for a variable
P_{01} , psia	98.61	P_{01}	0.55	64.37	P_{01}	0.02	2.74
P_{02} , psia	59.72	$P_{01} P_{01}$	148.66		$P_{01} P_{01}$	6.34	
P_2 , psia	43.36	P_{02}	1.83		P_{02}	0.08	
α_2 , deg	68.96	$P_{02} P_{02}$	393.34		$P_{02} P_{02}$	16.50	
T_{01} , °R	555.67	$P_{01} P_{02}$	-485.06		$P_{01} P_{02}$	-20.53	
T_{02} , °R	507.78	P_2	0.12	13.01	P_2	0.02	1.95
\dot{W} , lbf/s	11.47	$P_2 P_2$	0.09		$P_2 P_2$	0.01	
Tq , ft-lbf	243.87	$P_{01} P_2$	-7.76		$P_{01} P_2$	-0.49	
N , rpm	3754.36	$P_{02} P_2$	12.60		$P_{02} P_2$	0.79	
η_{th}	0.6458	α_2	0.49		α_2	0.06	
$U\eta_{th}$	0.0011	$\alpha_2 \alpha_2$	12.52	22.59	$\alpha_2 \alpha_2$	1.89	0.10
$U\eta_{th}$, %	0.2	T_{01}	8.80		T_{01}	0.00	
η_{me} , measured torque	0.6034	T_{02}	13.06		$T_{01} T_{01}$	0.10	
$U\eta_{me}$	0.0051	$T_{01} T_{01}$	270.58		\dot{W}	83.38	
$U\eta_{me}$, %	0.8	$T_{02} T_{02}$	324.83		Tq	11.69	
—	—	$T_{01} T_{02}$	-594.68		N	0.12	
—	—	Sum	100.0	100.0	Sum	100.0	100.0

torque correction. The following sections will explain the results of the detailed uncertainty analysis and will show how these results can serve as a guide for determining the preferred efficiency method for particular test situations.

Thermodynamic Method

The efficiency uncertainty for the thermodynamic method at the OTTR ADP was much lower (0.2% in η) than the test program goal (1% in η). There were three primary reasons for the low uncertainty in efficiency. First, a general uncertainty analysis was done early in the test program. These results were used to determine the critical measurements and then to set calibration requirements and define test techniques to improve these critical measurements. Therefore, many of the uncertainty estimates were reduced based on information gained from the general analysis. Second, making 720 point measurements of P_0 and T_0 at the turbine inlet and exit significantly lowered the uncertainty of the efficiency. Third, the correlation between measurements also significantly lowered the uncertainty of the efficiency.

Intuitively, one would think that increasing the number of measurements would decrease the uncertainty, but this can also be explained by examining the uncertainty equations. In the past, the uncertainty analysis has used one value for P_{01} , P_{02} , T_{01} , and T_{02} ; therefore, there was one uncertainty term for each of these variables. The analysis presented here started with 720 measurements of each variable and averaged these 720 measurements to obtain P_{01} , P_{02} , T_{01} , and T_{02} ; therefore, there were 720 precision uncertainty terms and 720 bias uncertainty terms for each of these variables. There were also terms to account for the correlation between the point measurements of the same variable. Thus, terms 1–18 on the right-hand side of the $U_{\eta_{th}}$ equation replaced four terms in the general uncertainty analysis. One may think that, with so many additional terms, the uncertainty would surely increase, but that was not the case. The values of the partial derivative terms were much lower when multiple measurements were made; for example, a perturbation to 1 of 720 measurements (P_{02i}) used to obtain P_{02} has a much smaller effect on the result than a perturbation to the one value of P_{02} . As a result, the total of terms 1–18 on the right-hand side of the $U_{\eta_{th}}$ equation with their summations was less than the total of the four terms used in the past. Therefore, making multiple measurements to obtain the average values needed for the efficiency equations and including the averaging procedure in the uncertainty analysis greatly reduced the uncertainty in the turbine efficiency.

To further understand the importance of including the averaging procedure in the uncertainty analysis, remember that the turbine exit terms were mass averaged due to the large gradients in the flowfield. The measurements used to obtain the mass weighting factors and the mass averaging procedure were explicitly included in the uncertainty analysis procedure. If area averaging had been used at the turbine exit, an estimate of the error that this would create in the average values required for the efficiency equation would have been needed for each measurement. Including this elemental error source to account for the conceptual bias would have increased the uncertainty estimate for each measurement. It would also be very difficult to obtain a good estimate for this source without mapping the flowfield. Therefore, choosing the correct averaging procedure for the flowfield and then explicitly including this averaging procedure in the analysis greatly improved the integrity of the results.

Obviously, 720 measurements cannot be made for all turbine tests. Fortunately, 720 measurements will not be needed for most test situations. With the information given here, an analysis could be used in the planning phase of an experiment to investigate the optimum number of measurements needed to achieve a certain efficiency goal. The equations could be written to calculate the average parameters using a set number of measurements and averaging method. The number of measurements could then be varied. Comparisons of the results would show the effect of the number of measurements on the uncertainty in the efficiency. One must be careful, however, to appropriately adjust the uncertainty estimates for each measurement based on the averaging procedure used and the number of measurements. Remember, the elemental error due to averaging using a finite

number of measurements instead of integrating a continuous function was considered negligible relative to the other elemental sources when 720 measurements were made. In a situation with fewer measurements, this elemental source could be significant and, if so, must be included in the uncertainty estimate. Also, if area averaging is used in a flowfield with significant gradients, the uncertainty estimate for each measurement must be increased to account for the conceptual bias induced by the averaging technique.

For the detailed uncertainty analysis, correlation between point measurements of different variables was also considered (terms 19–25 in the $U_{\eta_{th}}$ equation). For the thermodynamic method, three of these correlation terms were negative: P_{01} with P_{02} , P_{01} with P_2 , and T_{01} with T_{02} (Table 2). Again, these correlation terms greatly reduced the overall uncertainty in the thermodynamic efficiency and must be considered in the analysis.

Examination of the UPC values in Table 2 shows that the correlation terms between the point measurements of the same variable were the major contributors to the thermodynamic efficiency uncertainty. However, the correlation terms between T_{01} and T_{02} as well as between P_{01} and P_{02} had the largest UPC values. Fortunately, these terms were negative, and their effect was to decrease the efficiency uncertainty. These results are reasonable because the temperature drop across the turbine (not the absolute inlet and exit temperatures) followed by the turbine pressure ratio (not the absolute inlet and exit pressures) are the keys to accurately determining the efficiency using the thermodynamic method.

The method used for the OTTR thermocouple static calibration provided the negative correlation terms that greatly reduced the efficiency uncertainty with the thermodynamic method. The inlet and exit thermocouples were all calibrated end-to-end in the test facility against the same standard, and the uncertainty of the standard was the dominant elemental error source.⁷ This calibration procedure forced correlation between the errors in the inlet and exit temperature measurements. These correlation terms were negative because the efficiency depends on ΔT , not absolute T_{01} and T_{02} . Therefore, using a calibration procedure that forced correlation between the inlet and exit temperature measurements greatly reduced the overall uncertainty in efficiency. This static end-to-end calibration was the key to the success of the thermodynamic method.

Similarly, the correlation terms for the inlet and exit total pressures due to using the same electronic pressure scanning system also reduced the efficiency uncertainty. Again, the pressure ratio is the key to determining the efficiency, not the absolute P_{01} and P_{02} ; therefore, the correlation terms are negative. This effect was not as dramatic as for the temperature measurements, but was important nonetheless.

Mechanical Method

The efficiency uncertainty for the mechanical method at the OTTR ADP, neglecting the tare torque, was also lower (0.8% in η) than the test program goal (1% in η). However, this uncertainty was not as low as for the thermodynamic method, and the uncertainty will increase when the tare torque uncertainty is included. The three primary elements used to explain the low efficiency uncertainty estimate for the thermodynamic method will be addressed for the mechanical method to allow a comparison of the two methods.

Again, a general analysis was used to determine the critical measurements and then to set calibration requirements and define test techniques to improve these critical measurements. Therefore, many of the uncertainty estimates were reduced based on information gained from the general analysis. The pretest work put into reducing the uncertainty of the critical measurements was the primary reason for the success of the mechanical method. The averaging of the 720 point measurements of P_{01} , P_{02} , and T_{01} and the correlation between measurements of different variables also reduced the uncertainty in the mechanical efficiency, but not as significantly as for the thermodynamic method. The reason for this is explained next.

The general analysis showed that, for the OTTR, the mass flow rate was critical to accurately determining efficiency with the mechanical method. This is verified by the UPC results from the detailed analysis (Table 2). The mass flow rate uncertainty was reduced

by the venturi calibration,⁶ but the 720 point measurements of P_{01} , P_{02} , and T_{01} and correlation between point measurements of different variables did not affect the mass flow rate uncertainty. Averaging of the 720 point measurements did slightly reduce the efficiency uncertainty, primarily due to the contribution of the turbine exit pressure, but the magnitude of the effect was not as large as for the thermodynamic method.

Correlation between measurements of different variables also reduced the efficiency uncertainty for the mechanical method. Two of these terms were negative, P_{01} with P_{02} and P_{01} with P_2 , thereby reducing the efficiency uncertainty. The mechanical method did not benefit from a third negative correlation term because T_{02} was not required for this method. Therefore, the benefit of the correlation terms on the efficiency uncertainty was not as great for the mechanical method as for the thermodynamic method.

Again, the analysis is not complete for the mechanical method; the problem of the tare torque correction remains. The uncertainty results given here only consider the uncertainty of the measured torque. Until a value for the tare torque is obtained and an uncertainty estimate for the tare torque is added to the analysis, this method cannot be fully evaluated.

Conclusions

The question of how to determine the preferred efficiency method for cold airflow turbine testing for particular test situations has not been addressed in the past literature. This paper addresses the problem by evaluating two common turbine efficiency methods both experimentally and using uncertainty analysis techniques. Enhanced uncertainty analysis tools were developed to evaluate the efficiency uncertainty for both methods. The results allow a comparison of the two methods from which conclusions can be drawn to guide in determining the preferred efficiency method for individual applications. Using the form of the equations developed in this work is essential to obtaining the correct efficiency uncertainty estimates and the correct percentage contribution terms so that the methods can be properly evaluated.

The thermodynamic method can be superior to the mechanical method for determining turbine efficiency. For the test case discussed, with its specific calibration procedures, data acquisition techniques, and data analysis procedures, the efficiency uncertainty was lower for the thermodynamic method. However, for this method to be successful, extreme care must be taken with the temperature measurements. The turbine inlet and exit thermocouples must be calibrated end-to-end in the test facility using the same reference standard to force correlation between the bias errors in the temperature measurements. For high Mach number flows, a calibration for recovery factor is also needed. Furthermore, for high-gradient regions, the data must be properly mass averaged. This requires additional measurements of static pressure and flow angle, and the probes used to obtain these measurements must be calibrated. The analysis procedures outlined should be used to evaluate the number of point measurements needed to meet the efficiency uncertainty test goal for each case. If careful probe calibration is possible and an adequate number of measurements can be made, the thermodynamic method is the method of choice.

In some cases, the mechanical method may be the best option. If the overall measurements of mass flow rate, torque, and speed are available, careful probe calibration and the time to make multiple point measurements may not be required. If the turbine inlet flow is fairly uniform so that mass averaging is not required, it should be possible to determine the inlet total pressure and temperature to a suitable accuracy with relatively few measurements. The exit total pressure is also required for total-to-total efficiency, but the methods outlined can be used to evaluate the relative importance of this measurement to the efficiency uncertainty and the number of point measurements required to meet the efficiency uncertainty test goal for each case. However, the mass flow rate measurement and the tare torque correction are critical for the mechanical method. To successfully use this method, care must be taken to accurately obtain the mass flow rate, and one must be able to determine the tare torque correction for rig losses to obtain accurately the torque value required for the turbine efficiency equation.

Appendix: Efficiency Uncertainty Equations

The equation for uncertainty in thermodynamic efficiency is as follows:

$$\begin{aligned}
 U \eta_{th}^2 = & \sum_{i=1}^{720} \left(\frac{\partial \eta}{\partial P_{01i}} P_{01i} \right)^2 + \sum_{i=1}^{720} \left(\frac{\partial \eta}{\partial P_{02i}} P_{02i} \right)^2 \\
 & + \sum_{i=1}^{720} \left(\frac{\partial \eta}{\partial T_{01i}} T_{01i} \right)^2 + \sum_{i=1}^{720} \left(\frac{\partial \eta}{\partial T_{02i}} T_{02i} \right)^2 \\
 & + \sum_{i=1}^{720} \left(\frac{\partial \eta}{\partial P_{2i}} P_{2i} \right)^2 + \sum_{i=1}^{720} \left(\frac{\partial \eta}{\partial \alpha_{2i}} \alpha_{2i} \right)^2 \\
 & + \sum_{i=1}^{720} \left(\frac{\partial \eta}{\partial P_{01i}} B_{P_{01i}} \right)^2 + \sum_{i=1}^{720} \left(\frac{\partial \eta}{\partial P_{02i}} B_{P_{02i}} \right)^2 \\
 & + \sum_{i=1}^{720} \left(\frac{\partial \eta}{\partial T_{01i}} B_{T_{01i}} \right)^2 + \sum_{i=1}^{720} \left(\frac{\partial \eta}{\partial T_{02i}} B_{T_{02i}} \right)^2 \\
 & + \sum_{i=1}^{720} \left(\frac{\partial \eta}{\partial P_{2i}} B_{P_{2i}} \right)^2 + \sum_{i=1}^{720} \left(\frac{\partial \eta}{\partial \alpha_{2i}} B_{\alpha_{2i}} \right)^2 \\
 & + 2 \sum_{i=1}^{719} \sum_{j=i+1}^{720} \left(\frac{\partial \eta}{\partial P_{01}} \right)_i \left(\frac{\partial \eta}{\partial P_{01}} \right)_j B_{P_{01i} P_{01j}} \\
 & + 2 \sum_{i=1}^{719} \sum_{j=i+1}^{720} \left(\frac{\partial \eta}{\partial P_{02}} \right)_i \left(\frac{\partial \eta}{\partial P_{02}} \right)_j B_{P_{02i} P_{02j}} \\
 & + 2 \sum_{i=1}^{719} \sum_{j=i+1}^{720} \left(\frac{\partial \eta}{\partial T_{01}} \right)_i \left(\frac{\partial \eta}{\partial T_{01}} \right)_j B_{T_{01i} T_{01j}} \\
 & + 2 \sum_{i=1}^{719} \sum_{j=i+1}^{720} \left(\frac{\partial \eta}{\partial T_{02}} \right)_i \left(\frac{\partial \eta}{\partial T_{02}} \right)_j B_{T_{02i} T_{02j}} \\
 & + 2 \sum_{i=1}^{719} \sum_{j=i+1}^{720} \left(\frac{\partial \eta}{\partial P_2} \right)_i \left(\frac{\partial \eta}{\partial P_2} \right)_j B_{P_{2i} P_{2j}} \\
 & + 2 \sum_{i=1}^{719} \sum_{j=i+1}^{720} \left(\frac{\partial \eta}{\partial \alpha_2} \right)_i \left(\frac{\partial \eta}{\partial \alpha_2} \right)_j B_{\alpha_{2i} \alpha_{2j}} \\
 & + 2 \sum_{i=1}^{720} \sum_{j=1}^{720} \left(\frac{\partial \eta}{\partial P_{01}} \right)_i \left(\frac{\partial \eta}{\partial P_{02}} \right)_j B_{P_{01i} P_{02j}} \\
 & + 2 \sum_{i=1}^{720} \sum_{j=1}^{720} \left(\frac{\partial \eta}{\partial P_{01}} \right)_i \left(\frac{\partial \eta}{\partial P_2} \right)_j B_{P_{01i} P_{2j}} \\
 & + 2 \sum_{i=1}^{720} \sum_{j=1}^{720} \left(\frac{\partial \eta}{\partial P_{01}} \right)_i \left(\frac{\partial \eta}{\partial \alpha_2} \right)_j B_{P_{01i} \alpha_{2j}} \\
 & + 2 \sum_{i=1}^{720} \sum_{j=1}^{720} \left(\frac{\partial \eta}{\partial P_{02}} \right)_i \left(\frac{\partial \eta}{\partial P_2} \right)_j B_{P_{02i} P_{2j}} \\
 & + 2 \sum_{i=1}^{720} \sum_{j=1}^{720} \left(\frac{\partial \eta}{\partial P_{02}} \right)_i \left(\frac{\partial \eta}{\partial \alpha_2} \right)_j B_{P_{02i} \alpha_{2j}} \\
 & + 2 \sum_{i=1}^{720} \sum_{j=1}^{720} \left(\frac{\partial \eta}{\partial T_{01}} \right)_i \left(\frac{\partial \eta}{\partial T_{02}} \right)_j B_{T_{01i} T_{02j}} \\
 & + 2 \sum_{i=1}^{720} \sum_{j=1}^{720} \left(\frac{\partial \eta}{\partial P_2} \right)_i \left(\frac{\partial \eta}{\partial \alpha_2} \right)_j B_{P_{2i} \alpha_{2j}}
 \end{aligned}$$

The equation for uncertainty in mechanical efficiency is as follows:

$$\begin{aligned}
 U\eta_{me}^2 = & \sum_{i=1}^{720} \left(\frac{\partial \eta}{\partial P_{01i}} P_{P_{01i}} \right)^2 + \sum_{i=1}^{720} \left(\frac{\partial \eta}{\partial P_{02i}} P_{P_{02i}} \right)^2 \\
 & + \sum_{i=1}^{720} \left(\frac{\partial \eta}{\partial T_{01i}} P_{T_{01i}} \right)^2 + \sum_{i=1}^{720} \left(\frac{\partial \eta}{\partial P_{2i}} P_{P_{2i}} \right)^2 \\
 & + \sum_{i=1}^{720} \left(\frac{\partial \eta}{\partial \alpha_{2i}} P_{\alpha_{2i}} \right)^2 + \left(\frac{\partial \eta}{\partial \dot{W}} P_{\dot{W}} \right)^2 + \left(\frac{\partial \eta}{\partial T_q} P_{T_q} \right)^2 \\
 & + \left(\frac{\partial \eta}{\partial N} P_N \right)^2 + \sum_{i=1}^{720} \left(\frac{\partial \eta}{\partial P_{01i}} B_{P_{01i}} \right)^2 + \sum_{i=1}^{720} \left(\frac{\partial \eta}{\partial P_{02i}} B_{P_{02i}} \right)^2 \\
 & + \sum_{i=1}^{720} \left(\frac{\partial \eta}{\partial T_{01i}} B_{T_{01i}} \right)^2 + \sum_{i=1}^{720} \left(\frac{\partial \eta}{\partial P_{2i}} B_{P_{2i}} \right)^2 \\
 & + \sum_{i=1}^{720} \left(\frac{\partial \eta}{\partial \alpha_{2i}} B_{\alpha_{2i}} \right)^2 + \left(\frac{\partial \eta}{\partial \dot{W}} B_{\dot{W}} \right)^2 + \left(\frac{\partial \eta}{\partial T_q} B_{T_q} \right)^2 \\
 & + \left(\frac{\partial \eta}{\partial N} B_N \right)^2 + 2 \sum_{i=1}^{719} \sum_{j=i+1}^{720} \left(\frac{\partial \eta}{\partial P_{01i}} \right)_i \left(\frac{\partial \eta}{\partial P_{01j}} \right)_j B_{P_{01i} P_{01j}} \\
 & + 2 \sum_{i=1}^{719} \sum_{j=i+1}^{720} \left(\frac{\partial \eta}{\partial P_{02i}} \right)_i \left(\frac{\partial \eta}{\partial P_{02j}} \right)_j B_{P_{02i} P_{02j}} \\
 & + 2 \sum_{i=1}^{719} \sum_{j=i+1}^{720} \left(\frac{\partial \eta}{\partial T_{01i}} \right)_i \left(\frac{\partial \eta}{\partial T_{01j}} \right)_j B_{T_{01i} T_{01j}} \\
 & + 2 \sum_{i=1}^{719} \sum_{j=i+1}^{720} \left(\frac{\partial \eta}{\partial P_{2i}} \right)_i \left(\frac{\partial \eta}{\partial P_{2j}} \right)_j B_{P_{2i} P_{2j}} \\
 & + 2 \sum_{i=1}^{719} \sum_{j=i+1}^{720} \left(\frac{\partial \eta}{\partial \alpha_{2i}} \right)_i \left(\frac{\partial \eta}{\partial \alpha_{2j}} \right)_j B_{\alpha_{2i} \alpha_{2j}} \\
 & + 2 \sum_{i=1}^{720} \sum_{j=1}^{720} \left(\frac{\partial \eta}{\partial P_{01i}} \right)_i \left(\frac{\partial \eta}{\partial P_{02j}} \right)_j B_{P_{01i} P_{02j}} \\
 & + 2 \sum_{i=1}^{720} \sum_{j=1}^{720} \left(\frac{\partial \eta}{\partial P_{01i}} \right)_i \left(\frac{\partial \eta}{\partial P_{2j}} \right)_j B_{P_{01i} P_{2j}} \\
 & + 2 \sum_{i=1}^{720} \sum_{j=1}^{720} \left(\frac{\partial \eta}{\partial P_{01i}} \right)_i \left(\frac{\partial \eta}{\partial \alpha_{2j}} \right)_j B_{P_{01i} \alpha_{2j}} \\
 & + 2 \sum_{i=1}^{720} \sum_{j=1}^{720} \left(\frac{\partial \eta}{\partial P_{02i}} \right)_i \left(\frac{\partial \eta}{\partial P_{2j}} \right)_j B_{P_{02i} P_{2j}}
 \end{aligned}$$

$$\begin{aligned}
 & + 2 \sum_{i=1}^{720} \sum_{j=1}^{720} \left(\frac{\partial \eta}{\partial P_{02i}} \right)_i \left(\frac{\partial \eta}{\partial \alpha_{2j}} \right)_j B_{P_{02i} \alpha_{2j}} \\
 & + 2 \sum_{i=1}^{720} \sum_{j=1}^{720} \left(\frac{\partial \eta}{\partial P_{2i}} \right)_i \left(\frac{\partial \eta}{\partial \alpha_{2j}} \right)_j B_{P_{2i} \alpha_{2j}}
 \end{aligned}$$

References

- ¹Horlock, J. H., *Axial Flow Turbines*, Krieger, Malabar, FL, 1966, pp. 29–45.
- ²Rodi, F., Varetto, M., and Tomat, R., "Low Pressure Turbine Testing," AGARD CP- 293, Oct. 1980.
- ³Hudson, S. T., "Improved Turbine Efficiency Test Techniques Based on Uncertainty Analysis Application," Ph.D. Dissertation, Dept. of Mechanical and Aerospace Engineering, University of Alabama, Huntsville, AL, April 1998.
- ⁴Hudson, S. T., and Coleman, H. W., "A Preliminary Assessment of Methods for Determining Turbine Efficiency," AIAA Paper 96-0101, 1996.
- ⁵Hudson, S. T., Johnson, P. D., and Branick, R. E., "Performance Testing of a Highly Loaded Single Stage Oxidizer Turbine with Inlet and Exit Volute Manifolds," AIAA Paper 95-2405, 1995.
- ⁶Hudson, S. T., Bordelon, W. J., Jr., and Coleman, H. W., "Effect of Correlated Precision Errors on Uncertainty of a Subsonic Venturi Calibration," *AIAA Journal*, Vol. 34, No. 9, 1996.
- ⁷Hudson, S. T., "Oxidizer Technology Turbine Rig (Model 551) Thermocouple Static Calibration Posttest Report," NASA/Marshall Space Flight Center Memo ED34(96-012), Feb. 1996.
- ⁸Hudson, S. T., "Oxidizer Technology Turbine Rig (Model 551) Temperature and Pressure Rake Dynamic Calibration Posttest and Analysis Report," NASA/Marshall Space Flight Center Memo ED34(96-038), June 1996.
- ⁹Hudson, S. T., "Oxidizer Technology Turbine Rig (Model 551) Three-Hole Probe Calibration Report," Marshall Space Flight Center Memo ED34-98-0009, Huntsville, AL, Jan. 1998.
- ¹⁰Glassman, A. J., *Turbine Design and Application*, NASA SP-290, 1972.
- ¹¹Coleman, H. W., and Steele, W. G., *Experimentation and Uncertainty Analysis for Engineers*, Wiley, New York, 1989.
- ¹²Coleman, H. W., and Steele, W. G., "Engineering Application of Experimental Uncertainty Analysis," *AIAA Journal*, Vol. 33, No. 10, 1995.
- ¹³Brown, K. K., "Assessment of the Experimental Uncertainty Associated with Regressions," Ph.D. Dissertation, Dept. of Mechanical and Aerospace Engineering, Univ. of Alabama, Huntsville, AL, Nov. 1996.
- ¹⁴Brown, K. K., Coleman, H. W., Steele, W. G., and Taylor, R. P., "Evaluation of Correlated Bias Error Effects in Experimental Uncertainty Analysis," *AIAA Journal*, Vol. 34, No. 5, 1996.
- ¹⁵Brown, K. K., Coleman, H. W., and Steele, W. G., "A Methodology for Determining Experimental Uncertainty in Regressions," *Journal of Fluids Engineering*, Vol. 120, No. 3, 1998.
- ¹⁶Huber, F. W., Johnson, P. D., and Montesdeoca, X. A., "Baseline Design of the Gas Generator Oxidizer Turbine (GGOT) and Performance Predictions for the Associated Oxidizer Technology Turbine Rig (OTTR)," Pratt and Whitney Aircraft, United Technologies Corp., SZL:38865.doc to Scientific Research Associates, Inc., West Palm Beach, FL, April 1993.
- ¹⁷Hudson, S. T., Johnson, P. D., and Wooler, A., "Baseline Design of the Oxidizer Technology Turbine Rig," *Proceedings of the Advanced Earth-to-Orbit Propulsion Technology Conference*, Huntsville, AL, May 1994.
- ¹⁸Bordelon, W. J., Jr., Kauffman, W. J., Jr., and Heaman, J. P., "The Marshall Space Flight Center Turbine Test Equipment; Description and Performance," American Society of Mechanical Engineers, Paper 93-GT-380, 1993.
- ¹⁹Ainley, D. G., "Estimation of the Change in Performance Characteristics of a Turbine Resulting from Changes in the Gas Thermodynamic Properties," National Gas Turbine Establishment, Farnborough, Memo M.118, Repts. and Memoranda 2973, England, UK, June 1951.
- ²⁰Hudson, S. T., and Coleman, H. W., "A Detailed Uncertainty Assessment of Methods Used to Determine Turbine Efficiency," AIAA Paper 98-2711, 1998.